Using SIR Model for Spread of Disease to Investigate the Effects of Community Sentiment on Transmission Rates During an Epidemic

Sahand Setareh, Huilin Han, Kiersten Johnson and Jiaxuan Zhang

sahand.setareh@colorado.edu | huilin.han@colorado.edu | kiersten.johnson@colorado.edu | jizh4220@colorado.edu

Abstract - Using a basic SIR model for spread of disease on network structure representations of communities, our research focuses on the community-wide behaviors and policies that can consequently impact transmission. The effects of vaccine distribution intervals and efficacy demonstrate the pivotal effect that a vaccination advent can have on hindering disease progression, regardless of community structure based on sentiment. Research was conducted on the impact of disease duration, analyzing the duration of local epidemic simulations and the consequential impact of community sentiment. Different network structures simulating dynamic in-person and remote instruction methods were modeled using a changing network structure that periodically altered the community and its constituent relationships. Later, we introduce an SIRVS-G model that expands on the base model and demonstrates super group flocking events and re-entry of susceptible individuals from the compartmental model, closely mirroring the present phenomena observed with SARS-COV-2.

I. INTRODUCTION

It is no secret that the field of Epidemiology has garnered widespread attention through the past couple of years. Not only has the advent of a global pandemic demonstrated the necessity of more in-depth mathematical modeling in this domain, it has also allowed experts and officials alike to make better-informed decisions and implement more effective policies in response to these events. As such, our research group found the idea of modeling an epidemic (later expanded to model SARS-COV-2 by extension) on a community level to be of shared interest. Focus points such as vaccine distribution, disease duration impacts, remote vs. in-person instruction methods, and periodic grouping events based on flocking dynamics are analyzed and reported on by team members.

II. BACKGROUND & RELATED WORK

SIR models have been used in the past to model epidemiology. Within the past year, some work has been done with an SIR model base for the transmission of COVID-19 [1]. Additionally, there are a variety of notable studies on the impact of community sentiment during epidemics regarding social distancing and infection rates [2]. This project also draws inspiration from an educational video that attempts to account for a wide range of factors not typically accounted for in base SIR models [3]. Central meeting places and transmission rates mimicking that of sanitation attitudes are a couple of expansions on the basic model performed in the video. SIR models share strong support among academic groups as being accurate through their abstraction of the nature of how a disease spreads, and this project aims to leverage various sources in order to create a feasible model that will provide further insights into the effect of community sentiment on transmission rates during an epidemic.

III. METHODS

The SIR model for spread of disease [1] is a compartmental epidemiological model that provides a framework for analysis. In this basic model, a community with a constant number of individuals is compartmentalized into three population subcategories: Susceptible (S), Infected (I), and Recovered (R). Those who are considered susceptible are candidates to be infected. Those infected are capable of spreading the disease to those who are susceptible. Lastly, the population that has recovered are individuals who have been infected and then recovered from the disease. The rate of transmission is governed by parameters β and γ, where β is the infection rate per S-I contact and γ is the infection recovery rate per I-R (Fig. 1a).

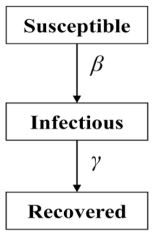

$$\frac{dS}{dt} = -\beta SI$$

$$\frac{dI}{dt} = \beta SI - \gamma I$$

$$\frac{dR}{dt} = \gamma I$$

Fig 1a. Rate of change of each SIR Compartment

It is important to note that transition rates β and γ are representational probabilities of contracting and recovering from conditions, and these subsequent transition rates are interpreted as probabilities with the range $0 \leq \beta \leq 1$ and $0 \leq \gamma \leq 1$.

A network representation of a community can appropriately define models such as social interactions and relationships within the community. This form of community representation draws inspiration from a similar study [4] that demonstrates disease progression dynamics on an SIR-network model. We start by building a network in which each member of the community is represented by a node and each interaction among each member that can result in transmission is defined as an edge in the said network. As the model progresses through iterations of time steps, there is a probability that an infected node will infect any neighboring nodes that share an edge, which is influenced by the aforementioned β rate of transmission. The parameter γ, or rate of recovery, determines the rate at which infected nodes will become recovered and removed from being able to be infected again.

Our study specifically focuses on the family-based network structure with each cluster of nodes representing each family in the community and all nodes in one family are connected to each other, which is represented by the caveman graph structure. We use average nodes of six to consist of a family (caveman graph) and connect all clusters of caveman graphs into two network structures: the connected caveman network and the relaxed caveman network (Fig 1b).

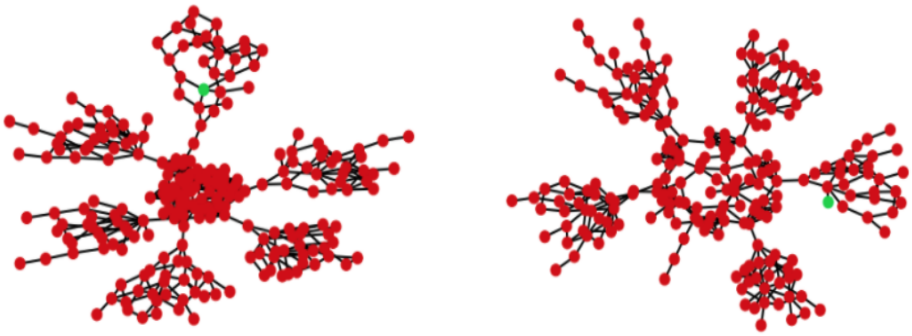

Fig 1b. Example of a connected caveman and relaxed caveman network structure featuring six defined clusters generated with gaussian random partition, with an initial infectious node depicted as the color green. Unlike Connected Caveman networks, Relaxed caveman models have probabilities associated with their edges.

IV. RESEARCH FOCUSES

Vaccine Distribution

Vaccines not only serve as monumental breakthroughs in the fight against real-world infectious diseases, but they also serve to inhibit a pathogen's transmission within our network structure as well. The approach to modeling vaccine distribution is constituted by a few generalizations. At some non-initial timestep, a vaccine is distributed to nodes within the community network structure at random, then subsequently deployed among random nodes again, iteratively over the course of a constant multiple of timesteps. Lastly, vaccines have an efficacy probability, that is to say there is a chance that a node will actually become vaccinated and immune from infection. Consequently, implementing the vaccine into the base SIR model effectively transforms the compartmental community into an SIRV model, whereby the susceptible nodes in the population that have received the vaccine are effectively inhibiting certain avenues of transmission within the community network structure.

A. Distribution Intervals

Using an initial SIRV model with corresponding $\beta = 0.6$ and $\gamma = 0.3$ parameters, the process was repeated for both connected caveman and relaxed caveman networks (Fig 1b) for vaccine distribution intervals at every seventh and fourth timestep. It is important to note that these parameters make for an aggressive, contagious pathogen to which vaccines will attempt to alleviate community-wide pressure.

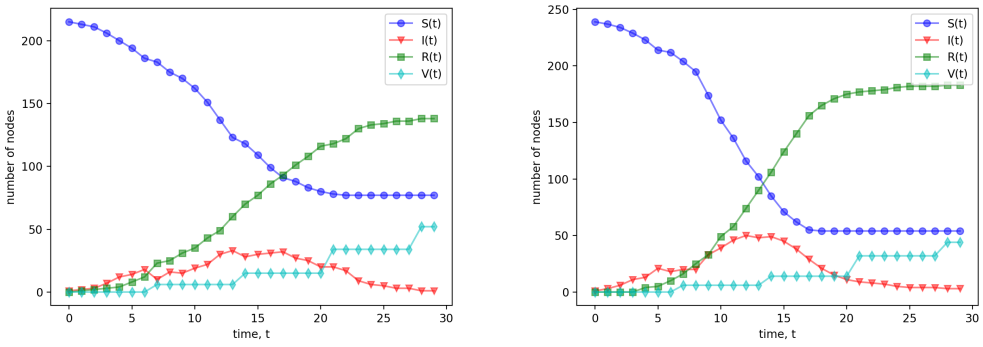

Fig 2. Vaccine distribution at every seventh time step for connected caveman and relaxed caveman graphs

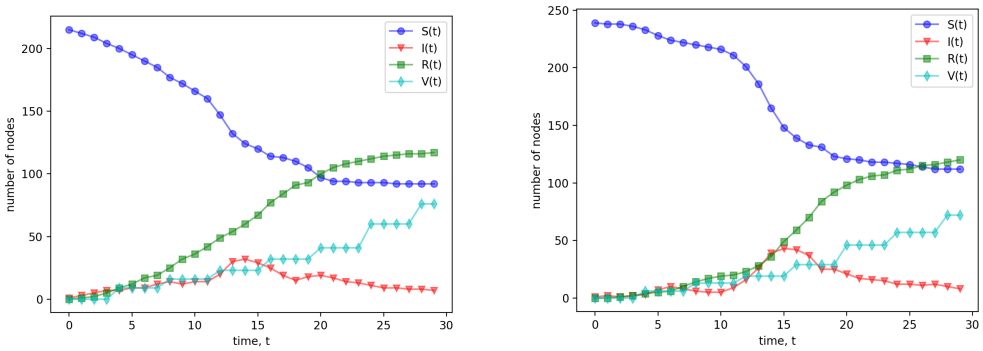

Fig 3. Vaccine distribution at every fourth time step for connected caveman and relaxed caveman graphs

The aggressive nature of the infectious disease given the aforementioned parameters $\beta = 0.6$ and $\gamma = 0.3$ is seen above. Both communities seem to experience a gradual rate of infection that climbs to a peak around timestep 15 before declining gradually as the number of susceptible individuals decreases at a rapid rate. The number of susceptible individuals plateaus after either a) there are no more individuals to infect within a particular community cluster or b) the vaccine has successfully created stopgaps in the network structure and has effectively blocked infected nodes from successively passing the infection to clusters or larger segments of the population.

There is a noticeable difference in transmission rates between the connected caveman and relaxed caveman network structure, as the former community has a much lower rate of infection as a function of time compared to that of the relaxed caveman structure (Fig. 2) as can be evidenced by the plateauing number of susceptible nodes. With a lower frequency of distribution, we see an interesting phenomena: the relaxed caveman structure suffers greatly from the lack of stopgaps in the network to inhibit transmission, while the connected graph suffers less intensely. In the case of more frequent vaccine distributions (Fig. 3), both the connected and the relaxed graphs benefit from the rapid introduction of vaccinated nodes to block avenues of transmission within the community, with the ending number of susceptible nodes higher than the seven-day distribution pattern for the connected caveman graph.

It is evident that vaccine distribution has a noticeable effect on the rate of infections, as all charts display a sharp decline in infections during second to third releases of vaccines. This demonstrates the potency of these network stopgaps and their ability to crush the progression of an infectious disease

B. Vaccine Efficacy

Running the same simulation for vaccine efficacy pairs of 0.75 and 0.8, and 0.9 and 0.95, for first and second doses respectively, the following charts depict the resulting progression of the SIRV model for a constant distribution interval of seven.

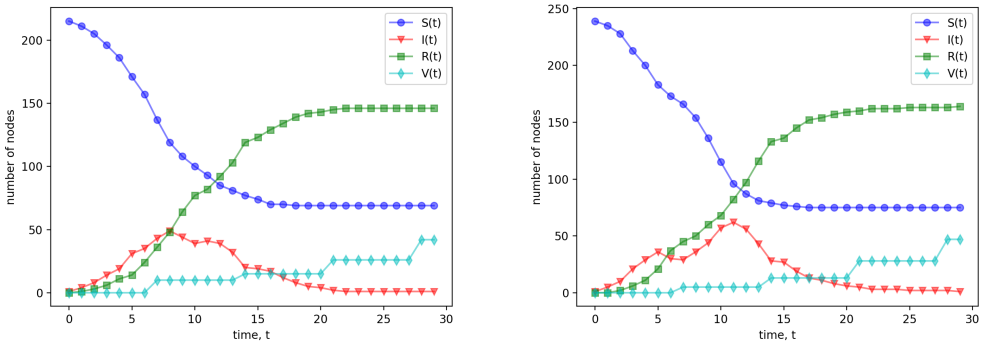

Fig 4. Vaccine efficacies of 0.75 and 0.80 for connected caveman and relaxed caveman graphs

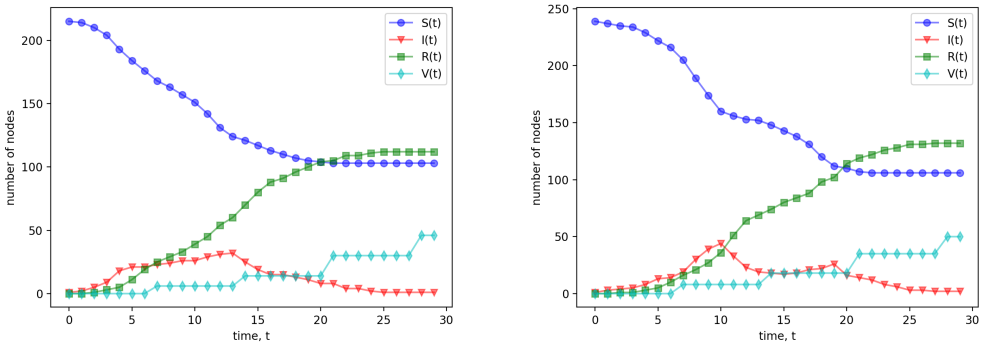

Fig 5. Vaccine efficacies of 0.90 and 0.95 for connected caveman and relaxed caveman graphs

When it comes to vaccine efficacy, lower probabilities demonstrate less potential for epidemic containment across both network structures (Fig 4). Higher vaccination efficacies are not as effective at limiting the spread of infections on a complex network structure like the relaxed caveman as higher vaccine distributions were (see Fig 3 and Fig 5). Higher vaccine efficiencies were most impactful on the less dense connected caveman graph, as any vaccination has a greater potential to stop the network-wide spread (Fig 5).

Ultimately, the charts tell a convincing story that more frequent distribution periods coupled with higher vaccine efficacy alongside a community network structure minimizing interactions among clusters (the connected caveman) produces the most infection-limiting results. On large, complex networks such as the relaxed caveman, infections are less hindered by vaccination efforts and are consequently more overwhelming. This speaks to the importance that community-wide behaviors and policies seeking to minimize transmission avenues (edges) carry.

Disease Duration Impacts

The duration of the persistence of the disease greatly impacts the overall number of people who get the disease. The Kolmogorov, or master equation, contains the probabilities that the population will be in each possible state [5]. These probabilities depend on the population size, connections between people (edges in our network), and the β and γ parameters. This model becomes complicated very quickly, as the probability of transferring to every single state is calculated. A population of 7 people, all interconnected socially, were charted with this model and the results from varying the β and γ parameters were recorded and compared to real diseases of the past. This comparison was completed via the basic reproduction number, or R_0, can be calculated from β/γ [6]. Three different R_0 values were compared to show the distribution of the number of recovered and partially recovered individuals based on the number of time steps it takes to complete the simulation (Fig 6). The simulation is complete when there are no more infected nodes left. At this point, either the disease has run through the entire population (Fully Recovered), or the disease did not reach all members of the population (Partially Recovered) but has died out. In either case, there are no more infected individuals present.

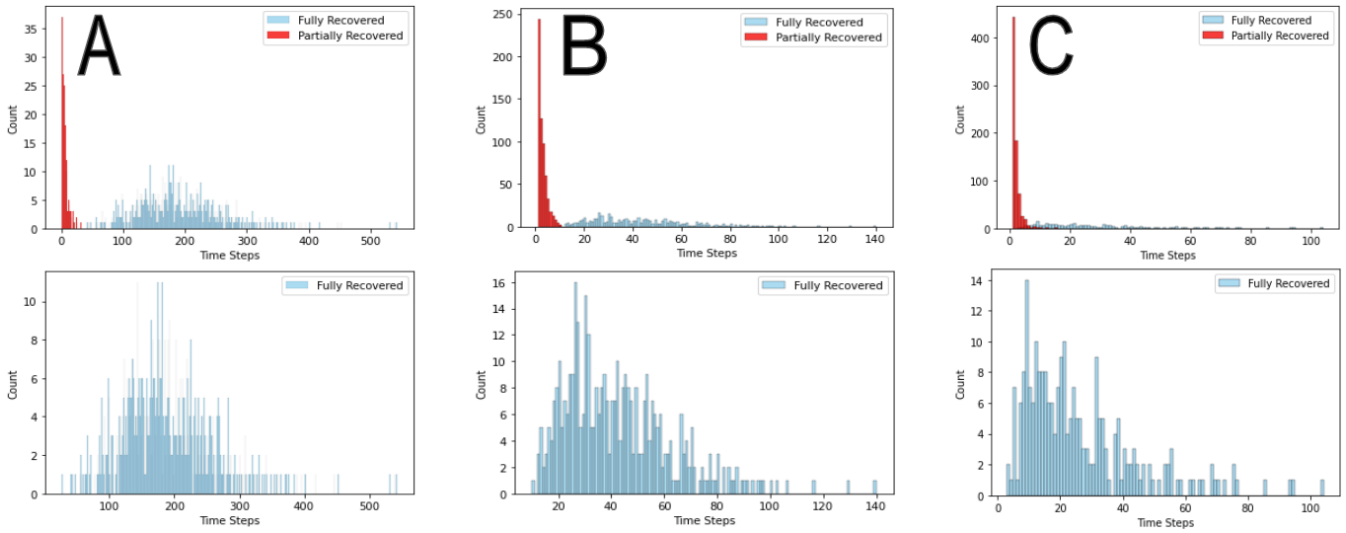

Fig 6. A) β=0.6; γ=0.04 ⟶ R_o=14.5, the same reproduction number as Measles; B) β=0.6; γ=0.24 ⟶ R_o=2.5, the same reproduction number as Covid-19; C) β=0.6; γ=0.45 ⟶ R_o=1.33, the same reproduction number as H1N1

Although this simulation only took 7 people into account, each scenario was for 1,000 runs which gave a fairly accurate general trend for the conditions. That is, with a higher rate of infection, β, relative to the recovery rate γ such as example in Figure 6A, the reproduction number is very high which leads to almost all of the scenarios ending with everyone having gotten and recovered from the disease. Also, the slow recovery rate leads to very drawn out total time steps. In contradiction, the examples with lower R_0 values have more scenarios where not all of the individuals within the population get the disease and it takes a much lower time for the disease to run its course. Typically, a higher R_0 value is thought to have a worse impact compared to a disease with a lower R_0 value, and thus should have more attention brought to the disease and to treating it [7]. This is true in that more people will likely get the disease and it will last longer. However, more analysis about the particular disease is needed to determine what is worse overall. For example, an influenza with an R_0 of 15 may still be a better scenario than a deadly virus with an R_0 of 1.5 due to the much worse (or even fatal) health impact the virus has on its victims. Thus, these sorts of analyses as displayed in Figure 6 only tell one side of the picture. As a note, any R_0 value greater than 1 is not good for the population as this indicates the disease is influenced to spread faster than individuals are recovering from it. Thus, if a disease was modeled with an R_0 value lower than 1 the time steps for the disease to go to completion would be very few, and the vast majority of cases would not infect all members of the population.

A somewhat similar analysis was completed on the SIRV model discussed in the Vaccine Distribution Research Focus section within this paper (Fig 7). This analysis shows the average proportion of people within the population that became infected and recovered from the disease in the course of the model and relates this to how many time steps it took the disease to run its course in the model. By looking at the first graph in Figure 7, it is apparent that a very low proportion of the population contracted the disease if it was only infecting people for less than 10 time steps. A slightly higher proportion contracted the disease if the model lasted between 10 and 15 time steps. After the model lasts longer than 15 time steps, the proportion of people who are infected shoots up to roughly 0.7 and stays around this value. The second graph in Figure 7 displays how many of the model runs occur within each time step. Slightly less than 1/10th of the runs finish their course in 6 or 7 time steps. However, the majority of the runs take between 20 and 30 time steps to run the course of the disease. Thus for the conditions tested with this model, for the majority of cases about 70% of the population will become infected. It should be noted that this network structure does not directly represent a real life epidemic example, but the general trends should hold true.

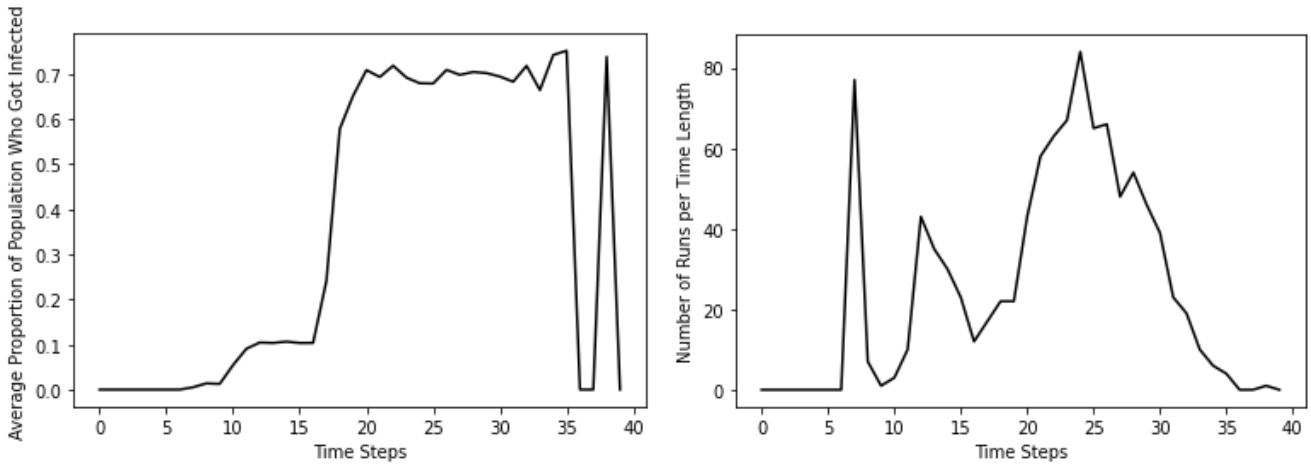

Fig 7. SIRV model results from over 1,000 runs. Graph one displays the average proportion of the population from the relaxed caveman graph which was infected by the end and charted it based on how many time steps the disease took to die out. Graph two displays the distribution of how many time steps it took the disease to die out.

Instruction Mode Shifting

Online university programs have existed for decades, but the COVID-19 pandemic turned remote learning into a common experience for college students in many countries around the world. At the onset of COVID-19 cases in the U.S, most universities made prompt decisions to move instruction fully remote to prevent the daily interactions on campus from aggregating the spread of disease. The speed of instruction mode shift was aided by the prevalence of computers and internet access among college students and staff and the availability of remote conference software. During the Spring 2020 semester, over 1,300 colleges and universities across the United States shifted from in-person classes to fully remote instruction. For the next fall, some universities decided to provide students with more learning modes and adopted hybrid plans of social-distancing in-person classes and remote learning. In fall of 2020, 44% of institutions remained remote, 21% were hybrid and 27% were fully in-person [8].

While remote instruction is the best guarantee for limiting disease spread amongst students, universities are eager to resume in-person instruction for many reasons. Students are showing a general sentiment of online learning fatigue, and studies have shown that "student performance, particularly for students who are already academically struggling, can suffer in online courses" [8]. Remote instruction mode also decreases the available work study jobs on campus, which many students depend on to support their studies. As a result of all the reasons above, universities will risk a drop in enrollment if they continue to plan for a mostly remote semester in fall of 2021, which will worsen the financial strain on universities which have already suffered from financial challenges since the start of the pandemic [8].

A concern for universities starting in person classes in the current times is the persisting high daily COVID-19 infection rates, and the uncertainty to the state of the pandemic when schools reopen in fall. As shown by examples in fall 2020, the increased on-campus and off-campus interactions when students move back to campus for in person classes result in a surge of COVID-19 cases throughout the student population. Many universities, including University of Colorado Boulder, chose to switch back to a fully remote instruction mode after COVID-19 cases in the community increased dramatically and local regulations tightened.

To investigate how switching between in person and remote instruction methods impacted the spread of cases, we need a way of simulating both instruction methods that builds on our SIR model. In person instruction methods are different from remote instruction due to the increased connection and proximity among student populations, therefore we used a change in network structure, specifically network connectivity, to model the two modes of instruction. During remote instruction, students mostly make contact with a small group of roommates and close friends, so our remote structure is characterized by small family structures that are loosely connected. The graph is made by loosely connecting seven connected caveman networks (Fig 7a).

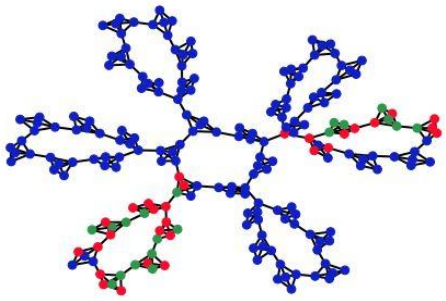

Fig 7a .Remote network structure

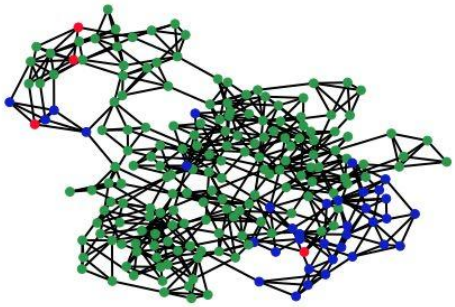

Fig 7b. In person network structure with 25% local connections and 10% global connections added to remote network structure

When we switch to in-person instruction, we add more connections upon the existing network. We add two types of connections: local and global (Fig 7b). Local connections simulate the increased connections within a close-knit community in the in-person instruction mode, global-connections simulate the extra connections throughout campus as a result of in-person, including classes, in-person jobs, campus interactions and more. Local connections are added randomly to a number proportional to the number of nodes in each connected caveman community, and global connections are added randomly to a number proportional to the number of nodes in the entire map.

The proportion of these random connections are parameters that can be changed, creating different levels of campus connectivity. In all simulations, the campus starts in an in-person state, and transitions to a remote state when the infections surpass a certain percentage. If the infections drop below another percentage in a remote state, the campus transitions back to an in-person state. The transition infection rates are also parameters to investigate.

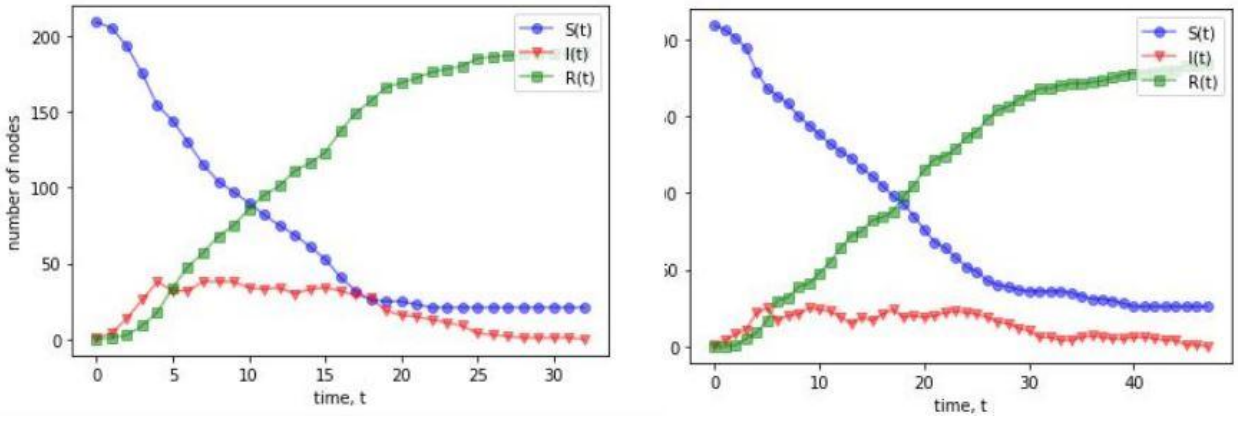

Figure 7c. Examples of the SIR model with instruction mode shift to remote and back to in-person triggered by infection rates of 10% and 2%, and with $\beta = 0.6$, $\gamma = 0.3$. The two graphs show a comparison over in-person connection density, with the image on the left having a 0.5 proportion of local connections and 0.2 of global connections, while the graph on the right has proportions of 0.25 local connections and 0.1 global connections.

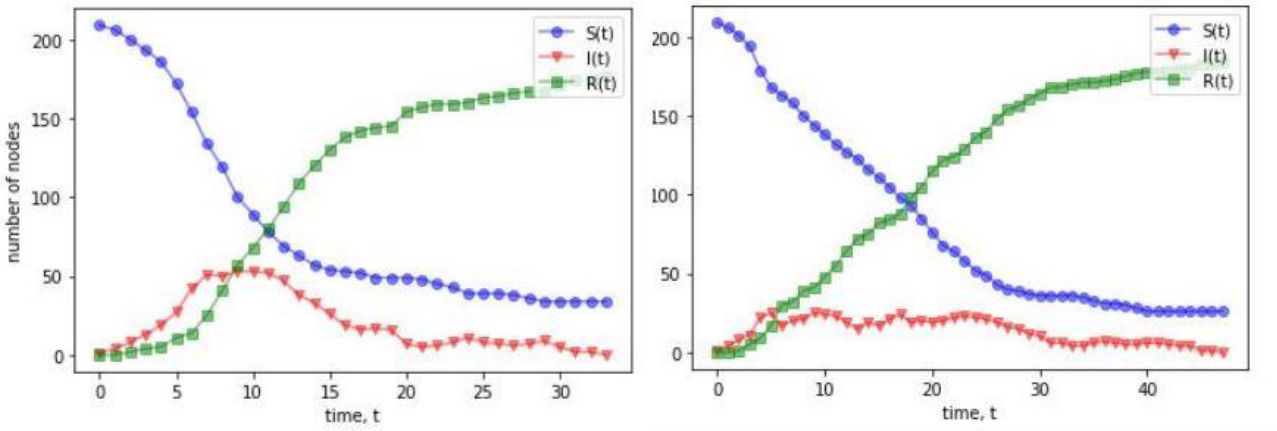

Figure 7d. Comparison of different thresholds of infection rates for switching from in-person to remote, with $\beta = 0.6$, $\gamma = 0.3$, threshold of switching from remote back to in-person at 2% infection rate, and local and global connection proportions of 0.25 and 0.1. The left graph shows a simulation where the threshold of switching to remote is an infection rate over 20%, where on the right the threshold is 10%.

In Figure 7c, the left graph with high proportions of additional in-person connections shows higher rates of infection towards the beginning of the simulation when the network is in an in-person state, and after switching to remote the high infection rates are sustained for a long time. This shows that even in an in-person state, reducing the overall risk-containing interactions can reduce the infection rates, and high connectivity in an in-person network will result in high rates of infection permeating through the network even after switching to remote. In Figure 7d, despite the higher threshold resulting in a larger peak of cases on the left graph, on both graphs the infection spread is halted by the switch to remote, and the rest of the graph is fairly similar on both sides. This indicates that switching fully to remote is very effective in preventing further increase of infection rates. This model has been helpful in showing the basic effectiveness of switching between in-person and remote instruction for slowing wide-spread campus infections, and in the future it would be interesting to run simulations on networks that are closer models of the university campuses, with a larger student population and have the additional connections in in-person mode more closely resemble the size and number of classes and activities an average student participates in.

Super Grouping Effect

Currently India is experiencing a tremendous outbreak of SARS-COV-2 and its new variant B.1.617 which is possibly due to their recent gatherings for the Kumbh Mela festival. On the festival's second-holiest day, April 12, India's Health Ministry reported nearly 170,000 new coronavirus infections. Nonetheless, on May 1, only less than two weeks after the gatherings, the number has gone over 300,000 per day causing more than 2,000 death cases per day. According to the report, almost 3 million Hindu pilgrims bathed in the Ganges River for the Kumbh Mela festival [9][10]. The Kumbh Mela festival might not be the sole cause of the surge of SARS-COV-2 in India but it clearly played a significant role in spreading the virus. Although there have not been any gatherings larger than the Kumbh Mela festival, political rallies, music festivals, or even large college parties might bring similar effects since these events shared one feature: an increased contact rate, which can dramatically increase the spreading of SARS-COV-2 and any new variants of the virus. We label this kind of event as the **Super Grouping Effect (SGE)** and in the model, **SGE** is represented by the increased edges among different clusters of nodes in a short period of time.

Based on the SIRV model, we add two new parameters: δ, which represents the re-susceptible rate per R-S since there might be a possibility of re-infection from the recovered population group, and there might also be a missing SARS-COV-2 test result due to the test sensitivity and test frequency [11]; and θ, which represents the amount of increased edges for each node in the network. This new model is named the SIRVS-G model. Using the parameters $\beta = 0.6$, $\gamma = 0.3$, $\delta = 0.4$, $\theta = 1$, we run multiple simulations of the new model SIRVS-G and the SIRVS model without **SGE** to compare and investigate how dramatically the increased virus transmission **SGE** can cause on the family based model. Examples of simulation results are shown in Fig 8.

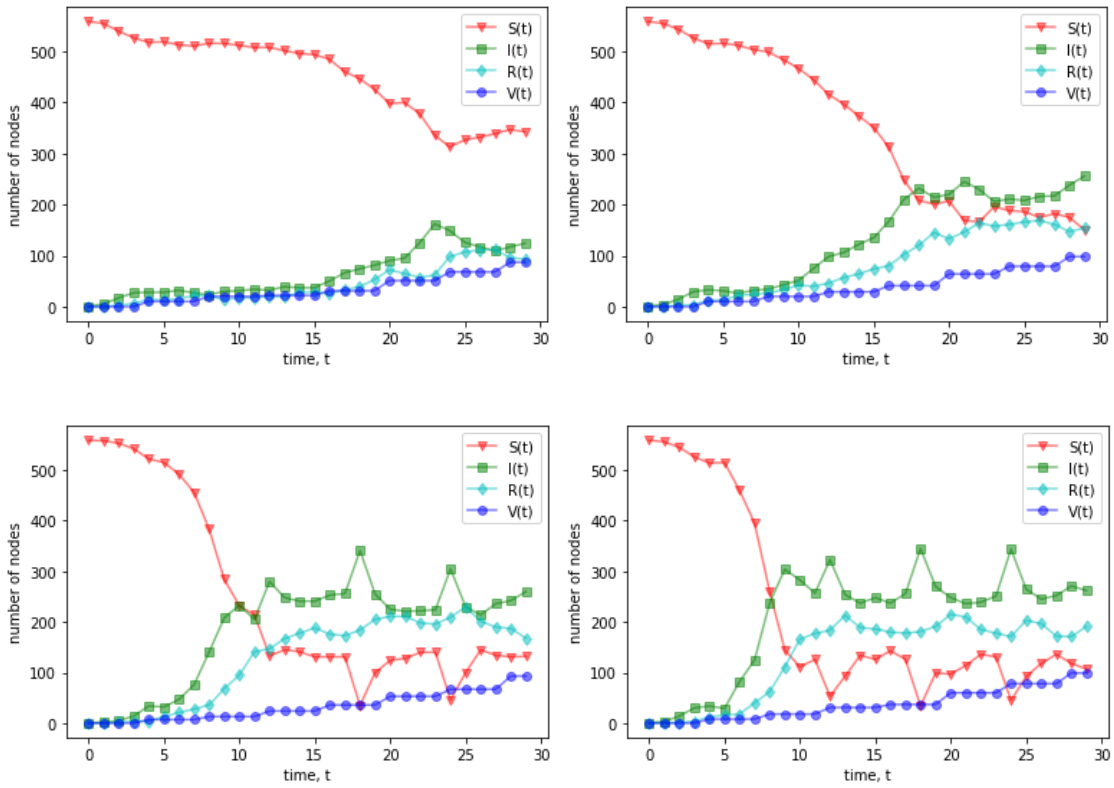

Fig 8. Examples of the comparison between the SIRVS-G model and SIRVS model, with parameters $\beta = 0.6$, $\gamma = 0.3$, $\delta = 0.4$, $\theta = 1$. Both model simulations run in the same network with 560 nodes and mean degree approximately equals 5. Both model simulations last for 30 days ($t = 30$). **SGE** is applied into the SIRVS-G simulation every six days meaning one super grouping event per week. The top panel represents the simulation results of the SIRVS model where the increase of infected population is smooth and steady. The bottom panel represents the simulation results of the SIRVS-G model where the increase of infected population is more dramatic and every time **SGE** is applied, the infected population reaches a new peak.

As shown in Figure 8, **SGE** increases the final infected population from a lower bound of 110 to an upper bound of 310 which is almost 3 times of the SIRVS infected population. Compared to the total number of nodes in the network which is only 560, less than two times of 310, the fraction of infected population over the total population increases from approximately 0.25 to over 0.5. Nonetheless, **SGE** generates a new peak of the total infected nodes which can significantly increase the virus transmission within the network since the infection rate is unchanged, the total amount of infected nodes is increased, the total amount of new infected nodes will also be increased. This kind of drastic infection is extremely powerful in the early stage of virus transmission since in the early stage, there have not been enough vaccines distributed to the majority of the community, once **SGE** is applied into the network, it is hard to stop the increase of infection.

The above simulations are run with $\theta = 1$ meaning every node increases one edge to any of other unconnected nodes. We modify this parameter into two edges increased for every node ($\theta = 2$) and we do not change other parameters, which means each node is interacting with one more node on average when **SGE** is applied. The example of simulation results are shown in Figure 9.

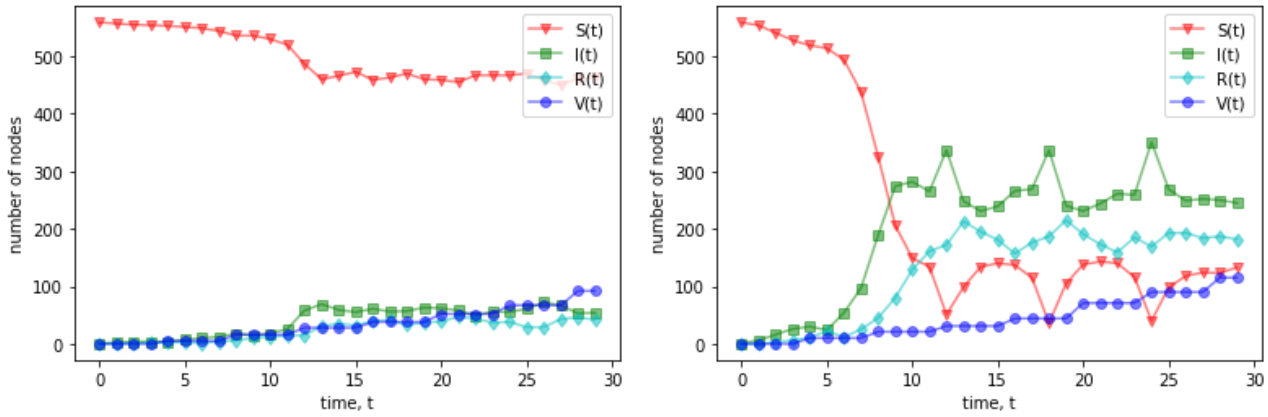

Fig 9. Examples of the comparison between the SIRVS-G model and SIRVS model, with parameters $\beta = 0.6$, $\gamma = 0.3$, $\delta = 0.4$, $\theta = 2$. Both model simulations run in the same network with 560 nodes and mean degree approximately equals 5. Both model simulations last for 30 days ($t = 30$). **SGE** is applied into the SIRVS-G simulation every six days meaning one super grouping event per week. The left panel represents the simulation results of the SIRVS model where the spread of infection is hindered. The right panel represents the simulation results of the SIRVS-G model where the increase of infected population is more dramatic and every time **SGE** is applied, the infected population reaches a new peak.

As shown in Figure 9, the infected population reaches a higher global maximum when $\theta = 2$ than when $\theta = 1$, meaning the largest amount of infected population is increased with the increased amount of interactions on average. The reason why the recovered population follows a similar increasing trend as the infected population is because we do not implement the method of delayed recovery from the infection meaning once the node is infected, there is a possibility of this node recovers on the second day of infection which is not likely to take place with SARS-COV-2 and its variants. Nevertheless, our model successfully simulates **SGE** on the social network. Even though the sizes and impacts of different super grouping events may be different, from the network structure perspective, they only differ from their θs, increased interactions of each individual in the events. Most importantly, all of them will significantly increase the virus transmission regardless of how effective current vaccines are. Once the infected population reaches a new peak, there is a high probability the virus will spread within the whole population just as what India is currently experiencing. More cases of B.1.617 have tested positive, the new variant SARS-COV-2 has been confirmed and there may be other highly-transmissible variants that we also need to pay attention to. With our SIRVS-G model and modifiable parameters, the approximate threshold numbers of any gatherings can be predicted and the consequent effects can be more easily studied.

V. BIBLIOGRAPHY

[1] Cooper, I., Mondal, A., & Antonopoulos, C. G. (2020). A SIR model assumption for the spread of COVID-19 in different communities. Chaos, solitons, and fractals, 139, 110057. https://doi.org/10.1016/j.chaos.2020.110057

[2] Zhou, J., Yang, S., Xiao, C., & Chen, F. (2020). Examination of community sentiment dynamics due to Covid-19 pandemic: A case study from australia. arXiv preprint arXiv:2006.12185.

[3] 3Blue1Brown (Director). (2020, March 27). Simulating an epidemic [Video file]. Retrieved March 28, 2021, from https://www.youtube.com/watch?v=gxAaO2rsdIs

[4] Chang, S. L., Piraveenan, M., & Prokopenko, M. (2019). The Effects of Imitation Dynamics on Vaccination Behaviours in SIR-Network Model. International journal of environmental research and public health, 16(14), 2477. https://doi.org/10.3390/ijerph16142477

[5] Keeling, M. J., & Ross, J. V. (2008). On methods for studying stochastic disease dynamics. *Journal of the Royal Society, Interface*, *5*(19), 171–181. https://doi.org/10.1098/rsif.2007.1106

[6] Ridenhour, B., Kowalik, J. M., & Shay, D. K. (2014). Unraveling R0: considerations for public health applications. *American journal of public health*, *104*(2), e32–e41. https://doi.org/10.2105/AJPH.2013.301704

[7] Linka, K., Peirlinck, M., & Kuhl, E. (2020). The reproduction number of COVID-19 and its correlation with public health interventions. *medRxiv : the preprint server for health sciences*, 2020.05.01.20088047. https://doi.org/10.1101/2020.05.01.20088047

[8] Smalley, A. (2021, March 22). Higher Education Responses to Coronavirus (COVID-19). https://www.ncsl.org/research/education/higher-education-responses-to-coronavirus-covid-19.aspx.

[9] Gettleman, J., Yasir, S., Kumar, H., Raj, S. (2021),The New York Times, As Covid-19 Devastates India, Deaths Go Undercounted, https://www.nytimes.com/2021/04/24/world/asia/india-coronavirus-deaths.html

[10] Pathak, S. (2021), Millions Flock To Hindu Festival Amid Coronavirus Spike, npr.org, https://www.npr.org/sections/coronavirus-live-updates/2021/04/13/986686352/millions-flock-to-hindu-festival-amid-coronavirus-spike

[11] Larremore, D. B., Wilder, B., Lester, E., Shehata, S., Burke, J. M., Hay, J. A., Tambe, M., Mina, M. J., & Parker, R. (2021). Test sensitivity is secondary to frequency and turnaround time for COVID-19 screening. Science Advances, 7(1), eabd5393. https://doi.org/10.1126/sciadv.abd5393

VI. PROJECT CONTRIBUTIONS

Sahand: I wrote the abstract, introduction, background and related work, and methods sections of the paper. I researched and presented findings on the vaccine distribution effects on the connected caveman and relaxed caveman network structures as detailed in the research focuses section (titled vaccine distribution). I also helped coordinate meetings and milestone progress updates.

Kiersten: I researched and presented findings on the timing distribution correlations among SIR and SIRV models. I solved the Kolmogorov equation to predict probabilities of each infection scenario. This section was titled "Disease Duration Impacts". I also edited and provided feedback on the work of others.

Hulin: I modeled and presented findings on the effects of instruction mode shifting on the spread of infectious disease through a university population, as detailed in the research focuses section (titled instruction mode shifting). I also built some networks structures that we used for our research focuses.

Justin: I built the basic SIR model template and implemented the **Super Grouping Effect (SGE)** aiming to study the disease spreading effect caused by events like the Kumbh Mela festival in India, music festivals, political rallies, and etc. A successful implementation can not only simulate the past experience of India, it can also provide insights into any other viruses such as the emerging B.1.617 variant of SARS-COV-2.